



## An MCell model of calcium dynamics and frequency-dependence of calmodulin activation in dendritic spines

Kevin M. Franks<sup>a,b,c,\*</sup>, Thomas M. Bartol<sup>a,c</sup>, Terrence J. Sejnowski<sup>a,b,c</sup>

<sup>a</sup>*Computational Neurobiology Laboratory, The Salk Institute, 10010 N. Torrey Pines Road, La Jolla, CA 92037, USA*

<sup>b</sup>*Department of Biology, University of California, San Diego, La Jolla, CA 92093, USA*

<sup>c</sup>*Howard Hughes Medical Institute, USA*

### Abstract

Pairing action potentials in synaptically coupled cortical pyramidal cells induces LTP in a frequency-dependent manner (H. Markram et al., *Science* 275 (1997) 213). Using MCell, which simulated the 3D geometry of the spine and the diffusion and binding of  $\text{Ca}^{2+}$ , we show that pairing five EPSPs and back-propagating action potentials results in a  $\text{Ca}^{2+}$  influx into a model dendritic spine that is largely frequency independent but leads to a frequency-dependent activation of postsynaptic calmodulin. Furthermore, we show how altering the availability of calmodulin and the calcium-binding capacity can alter the efficacy and potency of the frequency-response curve. The model shows how the cell can regulate its plasticity by buffering  $\text{Ca}^{2+}$  signals. © 2001 Elsevier Science B.V. All rights reserved.

*Keywords:* Calcium; Calmodulin; Buffering; Frequency-dependence; Long-term potentiation

### 1. Introduction

Hebbian synaptic plasticity in pyramidal neurons depends on the relative timing of presynaptic and postsynaptic activity [18]. Moreover, when action potentials are paired in synaptically coupled cortical neurons, long-term potentiation (LTP) is induced in a frequency-dependent manner [16]. Specifically, when 5 pairings of pre- and postsynaptic action potentials are presented at, or slower than, 5 Hz, no change in

\* Corresponding author. CNL, The Salk Institute, 10010 N. Torrey Pines Road, La Jolla, CA 92037, USA.

*E-mail address:* franks@salk.edu (K.M. Franks).

synaptic efficacy resulted, however 5 pairings at 10 Hz induces a persistent synaptic potentiation that increases with pairing frequency and saturated at 40 Hz. Calcium-calmodulin-dependent kinase II (CaMK II) in the postsynaptic density (PSD) is, at least initially, dependent on activated calmodulin (CaM) for its own activation, and implicated in the induction of LTP [12]. CaM activation requires the binding of four  $\text{Ca}^{2+}$  ions, and because CaM's affinity (17  $\mu\text{M}$ ) for  $\text{Ca}^{2+}$  is low relative to resting free intracellular  $\text{Ca}^{2+}$  concentration, typically around 50 nM, few of the sites are bound at rest [3]. When the cell is active,  $\text{Ca}^{2+}$  enters through either voltage- or ligand-gated channels [10]. CaM must compete with other intracellular  $\text{Ca}^{2+}$ -binding proteins (CBPs) for available  $\text{Ca}^{2+}$ , and only activates when all four sites are bound. Consequently, there is a highly non-linear relationship between  $\text{Ca}^{2+}$  influx and the activation of its downstream effectors.

If, for a given epoch of neural activity the total influx of  $\text{Ca}^{2+}$  is constant, then within a range, the total influx of  $\text{Ca}^{2+}$  depends linearly on the number of such epochs, but not on the frequency of their presentation; intracellular free  $\text{Ca}^{2+}$  concentration, however, is strongly dependent on pairing frequency [13]. First, the major source of  $\text{Ca}^{2+}$  in postsynaptic spines are NMDA channels [10,11], localized on the synaptic face [9], and  $\text{Ca}^{2+}$  diffuses through the cytoplasm from its site of entry. At high pairing frequencies,  $\text{Ca}^{2+}$  will accumulate near the NMDA channels before it has a chance to diffuse away. Second, pumps slowly return cytosolic  $\text{Ca}^{2+}$  concentration to resting levels by either pumping it out of the cell or sequestering it in intracellular stores [11]. The shorter the interval between successive pairings, less  $\text{Ca}^{2+}$  will have been pumped out of the cell since the previous pairing. Endogenous CBPs buffer free  $\text{Ca}^{2+}$ , but only indirectly affect the dependence of free  $\text{Ca}^{2+}$  concentration on pairing frequency. When  $\text{Ca}^{2+}$  first enters the spine it readily binds these proteins, however, their capacity saturates with sufficient  $\text{Ca}^{2+}$ , and the rate at which they recover is a function of both their  $K_{\text{off}}$  and the clearance rate via the pumps [13].

In this paper, we explore the relationship between  $\text{Ca}^{2+}$  dynamics (the activity-dependent influx of  $\text{Ca}^{2+}$  versus the cellular homeostatic mechanisms to maintain low levels of free intracellular  $\text{Ca}^{2+}$  and the activation of calmodulin, an intracellular  $\text{Ca}^{2+}$ -dependent effector protein. We first show how, for a given set of parameters, CaM activation is dependent on input-frequency. Then, by varying either the total amount of available CaM, or by changing the amount of CBPs, show how this frequency-dependence can be modulated. Previous models of  $\text{Ca}^{2+}$ -activation of calmodulin [6,7] are improved upon here by including individual channels rather than a non-specific  $\text{Ca}^{2+}$  flux into the cell and including the 3D-spatial organization of the spine. Furthermore, we include competition with other endogenous CBPs, where a previous model did not [6].

## 2. Methods

To examine the relationship between neural activity and CaM activation, we use MCell ([www.mcell.cnl.salk.edu](http://www.mcell.cnl.salk.edu)), a Monte Carlo simulator of microphysiology [2].

Briefly, this program allows for the 3D-simulation of  $\text{Ca}^{2+}$  diffusion by Brownian dynamics random walk and kinetic state transitions of channels and reactive molecules as diffusion-driven bimolecular associations and probabilistic, unimolecular Markov processes. Here, we model  $\text{Ca}^{2+}$  influx into a postsynaptic spine, modeled as a cube,  $0.5 \mu\text{m}$  along each side, and its binding to various intracellular proteins. Forty NMDA channels are placed on the synaptic face of the spine, and are gated by extracellularly released glutamate according to known rates [4]. High- (HVA) and low (LVA) voltage-activated  $\text{Ca}^{2+}$  channels are also placed at low densities on the spine membrane ( $1 \mu\text{m}^2$ ) [14]. Voltage commands for the open probability of the voltage-gated channels and the  $\text{Mg}^{2+}$ -block of the NMDA receptors are taken from an earlier model [15] using the NEURON simulation environment [5]. Once in the postsynaptic structure,  $\text{Ca}^{2+}$  can diffuse out of the spine through a neck at the bottom, bind to non-specific CBPs, be extruded or sequestered by pumps or can bind to, and activate, CaM. Four different types of CBPs were distributed throughout the spine. These molecules all bind  $\text{Ca}^{2+}$  with the same affinity ( $K_D = 1 \mu\text{M}$ ), but have different kinetics and concentrations: Fast-CBP,  $K_{\text{on}} 10^9 \text{M}^{-1} \text{s}^{-1}$ ,  $80 \mu\text{M}$ ; Medium-CBP,  $K_{\text{on}} 10^8 \text{M}^{-1} \text{s}^{-1}$ ,  $80 \mu\text{M}$ ; Slow-CBP,  $K_{\text{on}} 10^7 \text{M}^{-1} \text{s}^{-1}$ ,  $20 \mu\text{M}$ ; Very-slow-CBP,  $K_{\text{on}} 10^6 \text{M}^{-1} \text{s}^{-1}$ ,  $20 \mu\text{M}$  [17]. Calmodulin (CaM) was also included in the postsynaptic density (PSD), the top 50 nm of the spine, each of which could bind four  $\text{Ca}^{2+}$  ions according to experimentally determined rates [3]. Unless otherwise indicated, CaM concentration in the PSD was  $200 \mu\text{M}$ , corresponding to a total spine concentration of  $20 \mu\text{M}$ .

If a response were not frequency-dependent, its expected magnitude would be the product of the number of events and the magnitude of a single event. To determine the frequency-dependence of  $\text{Ca}^{2+}$  influx into the spine following five pairings, we computed the charge accumulation through HVA, LVA and NMDA channels by integrating each of their currents. These values are then normalized by five times the charge through each of the channel types following a single pairing. Similarly, frequency-dependence of  $\text{Ca}^{2+}$  concentration and CaM activation are determined by integrating the  $[\text{Ca}^{2+}]_i$  and  $[\text{CaM-4}]$  time series for each pairing frequency and normalizing by five times the respective values for a single pairing. Simulations were run on either PC workstations running FreeBSD 4.0 or on Bluehorizon, an IBM 1152-processor, massively parallel supercomputer, at the San Diego Supercomputer Center.

### 3. Results

To characterize the input frequency-dependence of calmodulin activation, we begin by simulating a single pairing of pre- and postsynaptic action potentials. The presynaptic action potential, represented as an excitatory postsynaptic potential (EPSP) in the postsynaptic cell, occurred 10 ms before the postsynaptic action potential (Fig. 1A). This generates an influx of  $\text{Ca}^{2+}$ , the details of which are described elsewhere (Franks et al., in preparation) Following a single pairing, most of the  $\text{Ca}^{2+}$

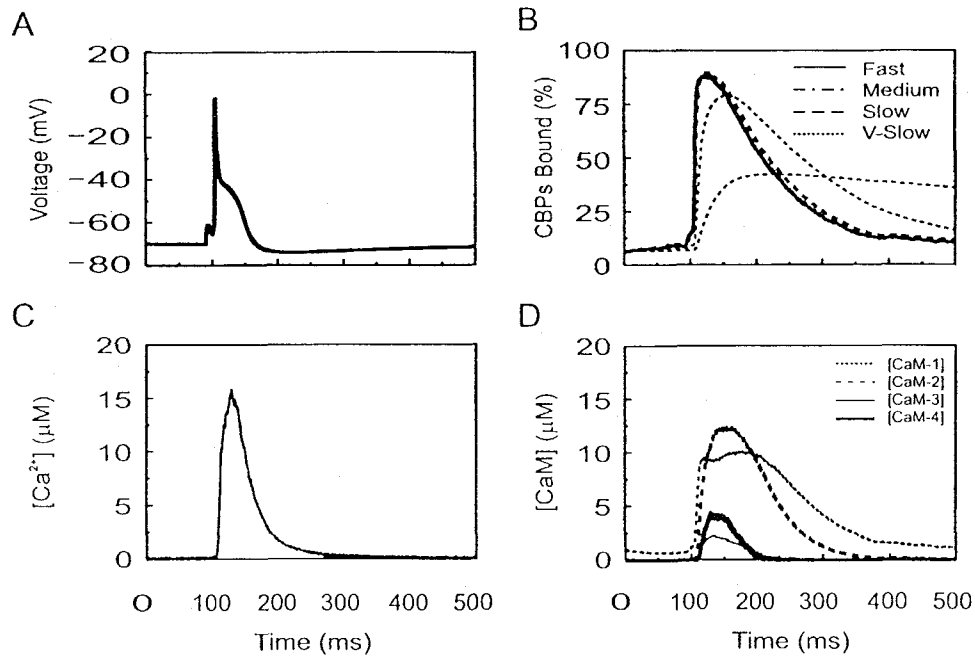


Fig. 1. A single EPSP and AP are paired, with the EPSP preceding the AP by 10 ms: (A) voltage trace, measured in the spine; (B) CBPs with different kinetics respond differentially to  $Ca^{2+}$  influx, (C) free  $Ca^{2+}$  concentration in the spine; (D) activation of CaM by  $Ca^{2+}$  binding. Calmodulin can be in a single, double, triple or, in its active, quadruple-bound form.

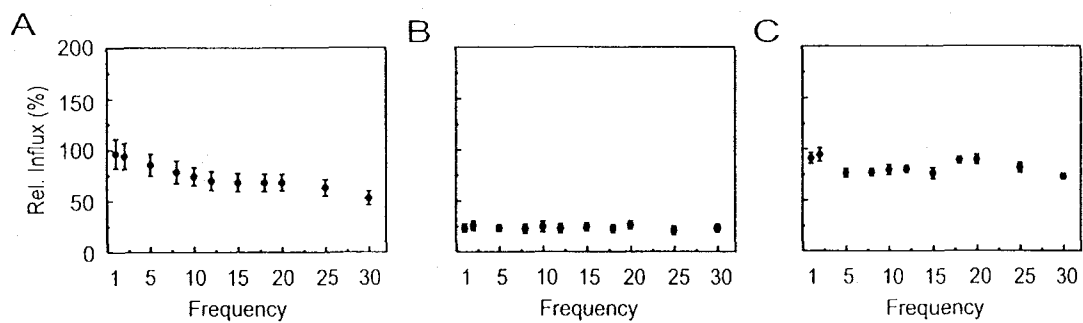


Fig. 2.  $Ca^{2+}$  influx is roughly frequency-independent: (A)  $Ca^{2+}$  influx from five pairings through HVA channels shows a modest frequency-dependence; (B) relative  $Ca^{2+}$  accumulation through LVA channels. These channels are largely activity-independent; (C) relative accumulation of  $Ca^{2+}$  through NMDA channels.

is buffered by CBPs, activating at different rates according to their kinetics (Fig. 1B). Some  $Ca^{2+}$  remains free, and a pairing results, on average, in peak free  $[Ca^{2+}]_i$  of approximately 16  $\mu M$  (Fig. 1C), corresponding to  $\sim 1200$  free  $Ca^{2+}$  ions in the spine head. Calcium also binds to CaM, in the PSD. Fig. 1D shows the different stages of  $Ca^{2+}$ -CaM binding, with, on average, about 5  $\mu M$  CaM activated by a single pairing.

Next, we presented five such pairings at frequencies ranging from 1 Hz to 30 Hz. Calcium influx through HVA channels is only slightly frequency-dependent (Fig. 2A).

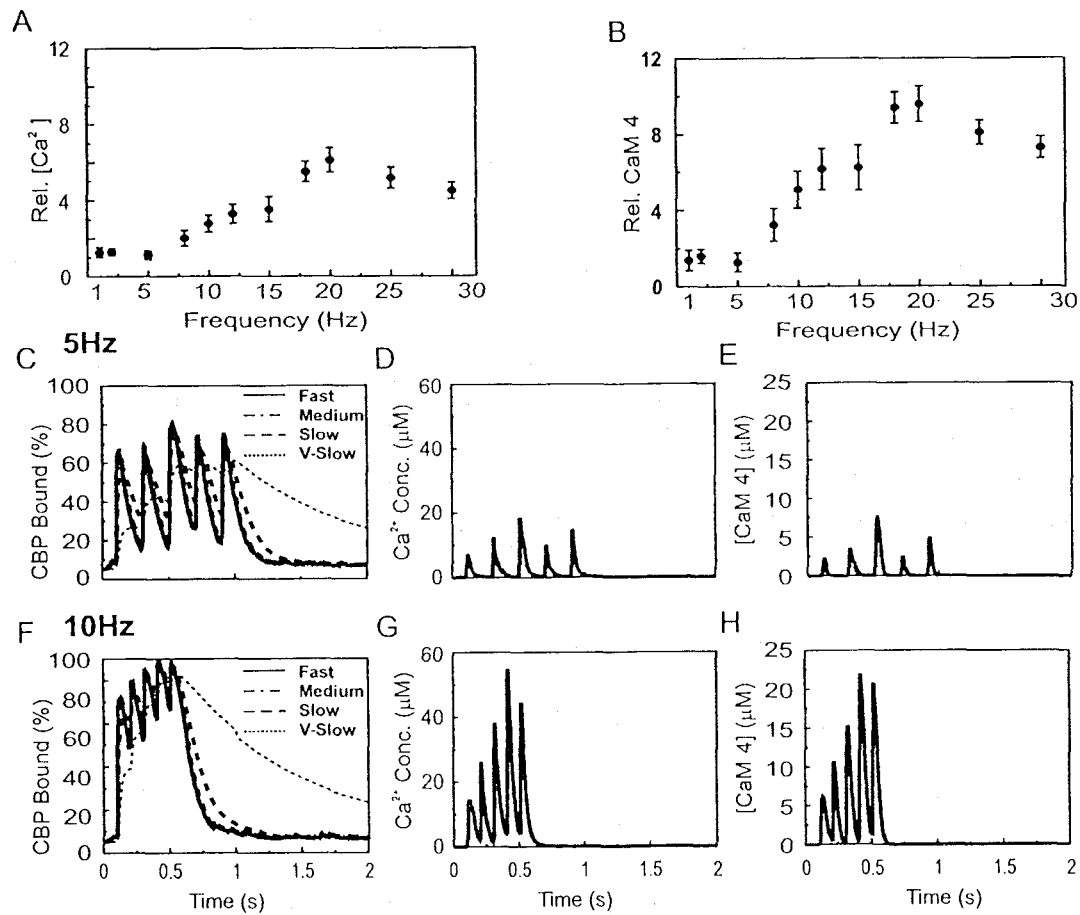


Fig. 3.  $\text{Ca}^{2+}$  concentration and activation of CaM-4 are strongly frequency-dependent: (A) frequency dependence of  $[\text{Ca}^{2+}]_i$  in the spine through a range of pairing frequencies; (B) frequency dependence of CaM-4 in the PSD; (C,F) Percentage of different CBPs bound during 5 and 10 Hz trains, respectively; (D,G)  $\text{Ca}^{2+}$  concentration in the spine during 5 and 10 Hz trains, respectively; (E,H) CaM-4 in the PSD during 5 and 10 Hz trains, respectively.

The modest frequency-dependent decrement in influx is due to channel inactivation (data not shown). Integrated and normalized LVA-mediated  $\text{Ca}^{2+}$  influxes have values of 0.2 for all frequencies (Fig. 2b), suggesting that  $\text{Ca}^{2+}$  influx through these channels is activity-independent. Indeed, current through these channels is almost negligible at a resting potential of  $-65$  mV, as most channels are inactivated at this potential (data not shown). Finally, charge through NMDA receptors is also only weakly frequency-dependent (Fig. 2C) due to both interference and receptor desensitization (data not shown).

Both  $[\text{Ca}^{2+}]_i$  and the quaternary-bound, activated form of calmodulin (CaM-4), on the other hand, are strongly frequency-dependent (Fig. 3A and B). The mechanisms underlying this result are shown to depend upon clearance rates and buffering capacities by comparing CBP occupation at two different frequencies. Following a train of pairings at 5 Hz, the CBPs track the  $\text{Ca}^{2+}$  influx and unload before the next

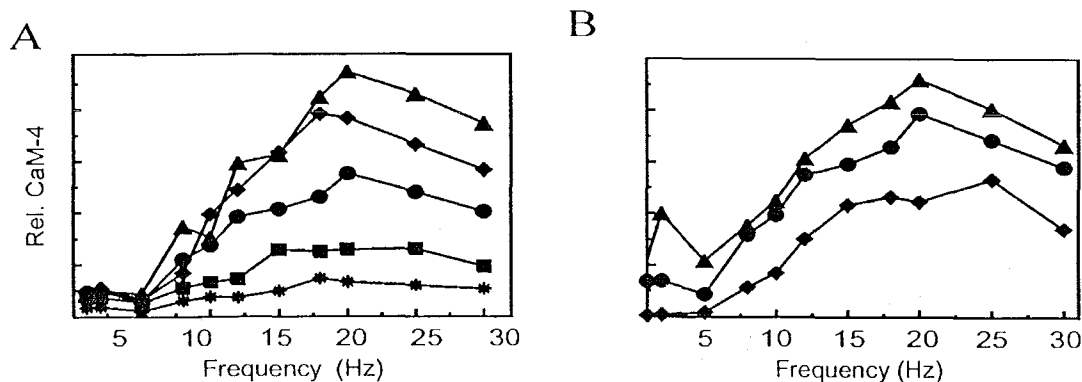


Fig. 4. Intracellular modulation of CaM activation: (A) shows the relation between  $[\text{CaM}]_{\text{total}}$  and frequency-dependence of CaM-4 activation. CaM concentrations in the PSD are: \*, 50  $\mu\text{M}$ ; ■, 100  $\mu\text{M}$ ; ●, 200  $\mu\text{M}$ ; ◆, 300  $\mu\text{M}$ ; ▲, 400  $\mu\text{M}$ . Total CaM-4 is expressed as integrated CaM-4 molecules over 5 s; (B) Increasing the concentration of CBPs shifts the frequency-dependent CaM-4 activation curve down and right. Total [CBP] in spine: ◆, 100  $\mu\text{M}$ ; ●, 200  $\mu\text{M}$ ; ▲, 400  $\mu\text{M}$ ; represented as integrated CaM-4 over 5 s.

pulse by releasing  $\text{Ca}^{2+}$  and allowing its extrusion from the spine (Fig. 3C). The unloading of the CBPs between successive pairings results in an approximately constant  $\text{Ca}^{2+}$  buffering capacity at each pairing, and consequently, little cooperativity in either  $[\text{Ca}^{2+}]_i$  or CaM-4 from pairing to pairing. Pairings at 10 Hz, however, rapidly saturate the buffering capacity of the CBPs as the pulses are presented before CBPs can unload from a previous pairing (Fig. 3F). Consequently, both  $[\text{Ca}^{2+}]_i$  (Fig. 3G) and CaM-4 (Fig. 3H) show strong cooperativity, where peaks in both  $[\text{Ca}^{2+}]_i$  and CaM-4 increase from pairing to pairing. Assuming identical initial conditions, the response to the first pairing should be identical for all pairing frequencies, and it is precisely the degree of cooperativity that endows the system its frequency dependence.

Finally, we further explore the frequency-response function for CaM-4; shown for one set of parameters in Fig. 3B. Total availability places a ceiling on the amount of CaM that can be activated. Changing the concentration of CaM in the PSD shifts the frequency-response curve up or down at high pairing frequencies (Fig. 4A). At saturating pairing frequencies the concentration of CaM-4 is proportional to the total concentration of CaM in the PSD. Changing the concentration of CBPs in the spine alters its  $\text{Ca}^{2+}$  buffering capacity. Halving or doubling CBP concentration shifts the frequency-response curve left and up, or right and down, respectively (Fig. 4B).

#### 4. Discussion

The buffering actions of other CBPs and the necessity of quadruple  $\text{Ca}^{2+}$  binding entail a low probability of activating CaM after a single pairing. Similarly, if repeated pairings are presented sufficiently far apart, both  $\text{Ca}^{2+}$  concentration and CBP occupancy will have returned to resting levels before each next pairing, and the

pairings are read as independent events. As the interval between pairings gets smaller, residual  $\text{Ca}^{2+}$  from previous pairings decrease competition for CaM and the probability of its activation increases. If enough pairings are presented at a sufficiently high frequency, all CaM will be activated and increasing pairing frequency will have no additional effect on CaM activation. If the amount of CaMKII activation is a predictor of LTP induction, and its activation is CaM-dependent, then the spatio-temporal activation of CaM will govern whether LTP will be induced. CaMKII's requirement for multiple activated CaMs and its concentration in the PSD make it sensitive to a rapid influx of  $\text{Ca}^{2+}$  through NMDA channels. Here, we show that CaM activation is dependent on the pattern of neuronal activity as well as the  $\text{Ca}^{2+}$  buffering capacity of other endogenous binding proteins. Thus by regulating the amount of CBPs, a cell can modulate the frequency sensitivity of CaM activation, and consequently, its LTP induction threshold [1]. Such modulation may partly underlie periods of enhanced plasticity in the developing nervous system [8].

### Acknowledgements

This work was supported by the NIH, NSF, Howard Hughes Medical Institute and the Human Frontier Science Program.

### References

- [1] W.C. Abraham, M.F. Bear, Metaplasticity: the plasticity of synaptic plasticity, *Trends Neurosci.* 19 (1996) 126–130.
- [2] T.M. Bartol Jr., B.R. Land, E.E. Salpeter, M.M. Salpeter, Monte Carlo simulation of miniature endplate current generation in the vertebrate neuromuscular junction, *Biophys. J.* 59 (1991) 1290–1307.
- [3] P. Cohen, C.B. Klee, *Calmodulin*, Elsevier, Amsterdam, New York, 1988.
- [4] N.A. Hessler, A.M. Shirke, R. Malinow, The probability of transmitter release at a mammalian central synapse, *Nature* 366 (1993) 569–572.
- [5] M.L. Hines, N.T. Carnevale, The NEURON simulation environment, *Neural Comput.* 9 (1997) 1179–1209.
- [6] W.R. Holmes, Models of calmodulin trapping and CaM kinase II activation in a dendritic spine, *J. Comput. Neurosci.* 8 (2000) 65–85.
- [7] W.R. Holmes, W.B. Levy, Insights into associative long-term potentiation from computational models of NMDA receptor-mediated calcium influx and intracellular calcium concentration changes, *J. Neurophysiol.* 63 (1990) 1148–1168.
- [8] L.C. Katz, C.J. Shatz, Synaptic activity and the construction of cortical circuits, *Science* 274 (1996) 1133–1138.
- [9] M.B. Kennedy, The postsynaptic density at glutamatergic synapses, *Trends Neurosci.* 20 (1997) 264–268.
- [10] H.J. Koester, B. Sakmann, Calcium dynamics in single spines during coincident pre- and postsynaptic activity depend on relative timing of back-propagating action potentials and subthreshold excitatory postsynaptic potentials, *Proc. Natl. Acad. Sci. USA* 95 (1998) 9596–9601.
- [11] Y. Kovalchuk, J. Eilers, J. Lisman, A. Konnerth, NMDA receptor-mediated subthreshold  $\text{Ca}^{2+}$  signals in spines of hippocampal neurons, *J. Neurosci.* 20 (2000) 1791–1799.

- [12] J. Lisman, The CaM kinase II hypothesis for the storage of synaptic memory, *Trends Neurosci.* 17 (1994) 406–412.
- [13] H. Maeda, G.C. Ellis-Davies, K. Ito, Y. Miyashita, H. Kasai, Supralinear  $\text{Ca}^{2+}$  signaling by cooperative and mobile  $\text{Ca}^{2+}$  buffering in Purkinje neurons, *Neuron* 24 (1999) 989–1002.
- [14] J.C. Magee, D. Johnston, Characterization of single voltage-gated  $\text{Na}^+$  and  $\text{Ca}^{2+}$  channels in apical dendrites of rat CA1 pyramidal neurons, *J. Physiol. (London)* 487 (1995) 67–90.
- [15] Z.F. Mainen, J. Joerges, J.R. Huguenard, T.J. Sejnowski, A model of spike initiation in neocortical pyramidal neurons, *Neuron* 15 (1995) 1427–1439.
- [16] H. Markram, J. Lubke, M. Frotscher, B. Sakmann, Regulation of synaptic efficacy by coincidence of postsynaptic APs and EPSPs, *Science* 275 (1997) 213–215.
- [17] H. Markram, A. Roth, F. Helmchen, Competitive calcium binding: implications for dendritic calcium signaling, *J. Comput. Neurosci.* 5 (1998) 331–348.
- [18] T.J. Sejnowski, The book of Hebb, *Neuron* 24 (1999) 773–776.



**Kevin Franks** received his B.Sc. Biomedical Science and B.A. in Philosophy from the University of Guelph in Canada. He is presently a doctoral candidate at University of California, San Diego, working in the Computational Neurobiology Lab at the Salk Institute. He is interested in the mechanisms by which synapses change their weights. On weekends, he tames lions and massages porcupines.



**Tom Bartol** is a research associate in the Computational Neurobiology Laboratory at the Salk Institute. He earned his Ph.D. in Neurobiology & Behavior in the laboratory of Miriam Salpeter at Cornell University. He is a co-author of the MCell Monte Carlo simulator of cellular microphysiology.



**Terrence Sejnowski** is an Investigator with the Howard Hughes Medical Institute and a Professor at The Salk Institute for Biological Studies where he directs the Computational Neurobiology Laboratory. He is also Professor of Biology at the University of California, San Diego, where he is Director of the Institute for Neural Computation. Dr. Sejnowski received his B.S. in Physics from the Case-Western Reserve University, M.A. in Physics from Princeton University, and a Ph.D. in Physics from Princeton University in 1978. In 1988, Dr. Sejnowski founded Neural Computation, published by the MIT Press. He is also the President of the Neural Information Processing Systems Foundation. The long-range goal of Dr. Sejnowski's research is to build linking principles from brain to behavior using computational models. This goal is being pursued with a combination of theoretical and experimental approaches at several levels of investigation ranging from the biophysical level to the systems level.